Selective chemical shift assignment of bacteriochlorophyll a in uniformly [C-13-N-15]-labeled light-harvesting 1 complexes by solid-state NMR in ultrahigh magnetic field

Pandit, A.; Buda, F.; Gammeren, A.J. van; Ganapathy, S.; Groot, H.J.M. de

Selective Chemical Shift Assignment of Bacteriochlorophyll *a* in Uniformly [^{13}C−^{15}N]-Labeled Light-Harvesting 1 Complexes by Solid-State NMR in Ultrahigh Magnetic Field

Anjali Pandit,* Francesco Buda, Adriaan J. van Gammeren,† Swapna Ganapathy, and Huub J. M. de Groot

Leiden Institute of Chemistry, Leiden University, P.O. Box 9502, 2300 RA Leiden, The Netherlands

Received: January 24, 2010; Revised Manuscript Received: March 25, 2010

Magic-angle spinning (MAS) ^{13}C−^{13}C correlation NMR spectroscopy was used to resolve the electronic ground state characteristics of the bacteriochlorophyll *a* (BChl *a*) cofactors in light-harvesting 1 (LH1) complexes of *Rhodopseudomonas acidophila* (strain 10050). The BChl *a* ^{13}C isotropic chemical shifts of the LH1 complexes are compared to the ^{13}C chemical shifts for BChl *a* dissolved in acetone-d_6 and to ^{13}C NMR data that has been obtained for the B800 and B850 BChl molecules in *Rps. acidophila* peripheral light-harvesting complexes (LH2). Since both complexes contain BChl *a* cofactors, we can address the chemical shift variability for specific carbon responses between the two types of antennae. The global shift pattern of the LH1 BChl's resembles the shift patterns of the LH2 α- and β-B850 BChl's, while some carbon responses, in particular the C3 and C3^1, show significant deviations. A comparison with density functional theory (DFT) shift calculations provides insight into the BChl concomitant structural and electronic interactions in the ground state. The differences in the LH1 BChl observed chemical shifts relative to the ^{13}C responses of BChl *a* in solution cannot be explained by local side chain interactions, such as hydrogen bonding or nonplanarity of the C3 acetyl, but appear to be dominated by protein-induced macrocycle distortion. Such shaping of the macrocycle will contribute significantly to the red shift of the BChl Q_y absorbance band in purple bacterial light-harvesting complexes.

Introduction

The processes of photosynthesis critically depend on higher-order interactions in tightly packed pigment−protein complexes that induce localized perturbations of their conformational and electronic structures. This way, functional activation mechanisms are established for tuning of the absorption wavelength for efficient light harvesting and to lower the barriers for charge separation and catalysis. The need to understand such activation mechanisms for the design of biomimetic artificial photosynthesis devices made us engage in a detailed investigation of the ground-state properties of bacterial light-harvesting antennae by solid-state NMR. By this technique, we aim to understand the interplay between the pigments and the surrounding protein environment in terms of concerted structural and electronic interactions, which appear as local perturbations in the pigment as well as in the apoprotein chemical shifts.[1,2]

In purple nonsulfur bacteria, sunlight is absorbed by the peripheral light-harvesting 2 complexes (LH2) and transferred to the core light-harvesting 1 complexes (LH1) that surround the photosynthetic reaction centers (RC).[3] The robustness of the purple bacterial pigment−protein assemblies, their high ring-shaped symmetry of repeating subunits, and their possibilities for guided self-assembly *in vitro*[4−7] make them of particular interest as templates for the construction of hybrid biomimetic devices.[8−10] The peripheral and core light-harvesting complexes have ring-shaped symmetries of heterodimer α- and β-polypeptide subunits. Each subunit binds two bacteriochlorophyll *a* (BChl *a*) pigments that form rings of pigment dimers, called the B870 and B850 band for LH1 and LH2, respectively, with interdimer overlap. Efficient energy transfer occurs among the ring of dimer BChl's through excitonic interactions that are responsible for the major part of the red shift in their Q_y optical absorption maxima.[11] The LH2 subunits bind a third BChl that forms a ring of BChl monomers, called the B800 band. In addition, each subunit binds a carotenoid molecule. For the LH2 complexes of *Rs. molischianum* and *Rps. acidophila*, high-resolution crystal structures have been determined.[12−14] In contrast, currently no high-resolution structure exists for LH1. A low-resolution structure has been obtained for the LH1−RC complex of *Rps. palustris* by X-ray diffraction techniques,[15] showing that the reaction center is surrounded by an oval, horseshoe-shaped, LH1 complex that consists of 15 pairs of heterodimer subunits. In addition, a single transmembrane helix is present that is equivalent to the pufX protein that has been found in LH1 antenna complexes of *Rb. sphaeroides* and *capsulatus*.[16−18] Closed symmetrical rings have been observed by AFM for core complexes of *Blastochloris viridis*,[19] and also in the low-resolution EM projection maps of LH1 complexes of *Rs. rubrum*.[20,21]

In addition to excitonic pigment−pigment interactions, the light-harvesting properties of the BChl's are tuned by the protein matrix.[22] The demonstrated flexibility of the LH1 in atomic force microscopy (AFM) and single particle analyses[23,24] can have an effect on the Q_y absorbance band. Recent calculations using a structural model of the dimeric RC−LH1−PufX complex of *Rb. sphaeroides* demonstrated that the S-shaped dimeric BChl

* Corresponding author. Present address: Dept. of Physics and Astronomy, Faculty of Sciences, VU University, De Boelelaan 1081, 1081 HV Amsterdam, The Netherlands. E-mail: apandit@few.vu.nl. Phone: +31 (0)20-5987937. Fax: +31(0)20-5987899.

† Present address: Amphia Ziekenhuis, Klinisch Chemisch en Hematologisch Laboratorium, Langendijk 75, 4819 EV Breda, The Netherlands.

10.1021/jp100688u
Published on Web 04/21/2010

array displays excitonic properties that are notably different from those of the circularly symmetric RC−LH1 monomeric complexes studied previously.[25] However, neither the bending of the BChl array nor the structural discontinuity that results from the gap caused by PufX had a significant effect, and the resonant energy transfer between peripheral antennae and RCs was mostly unaffected by the dimerization and the out of-plane distortion of the BChl array. On a molecular scale, several protein-induced parameters determine the BChl optical site energies. The BChl excitation energies depend on hydrogen bonding to the C3 acetyl, which induces a red shift of the BChl Q_y absorption band accompanied by a downshift of the acetyl Raman stretching mode.[26−29] In contrast, hydrogen bonding to the C13 keto carbonyl was found to have no spectral effect but affected the stability and assembly of LH2 complexes.[30,31] For porphyrin molecules, macrocycle distortion shifts the absorption spectrum and causes a major decrease of the lifetime of the first excited state.[32] Although the observed distortions of protein-bound BChl's are much smaller than the distorted porphyrin structures that have been addressed, the LH2 *acidophila* high-resolution crystal structures show that none of the BChl macrocycles is fully planar, with significant distortion of its βB850 BChl.[12,13] Raman experiments indeed revealed that the BChl macrocycles in LH2 and LH1 complexes are far from relaxed, with differences between the α- and β-BChl.[33] A mutation study replacing the BChl contact residues in *sphaeroides* LH2 revealed a linear relationship between the bulkiness of the residue side chains and a Q_y blue shift, suggesting that a change in packing leads to pigment displacements. [34] In addition, it was proposed that packing-induced macrocycle deformation promotes H-bonding to the C3 acetyl. The blue-shifted Q_y absorption of LH3 complexes grown under low-light conditions could not be fully explained by differences in H-bonding and macrocycle deformation between the LH3 and LH2 BChl's and was attributed to further out-of-plane rotation of the C3 acetyl side chain. [35] In the absence of a high-resolution structure of LH1, a very recent site-directed mutagenesis study on *sphaeroides* LH1 used modeled electronic structures of the LH1 BChl's to explain changes in the excitation energies in terms of H-bonding and rotation of the C3-acetyl. [36] Additional to H-bonding and structural effects, polarity of the protein environment can play a role and the electrostatics of the LH2 B800 environment induce a red shift of 160 cm^{-1} in the Q_y absorption of the B800 BChl's. [28]

Solid-state NMR provides a sensitive method to probe the local environment of the BChl cofactors with atomic selectivity. With the support of density functional theory (DFT) calculations, functional interactions between the BChl's and coordinating histidines have been revealed in the LH2 and RC complexes of purple bacteria.[37,38] The LH1 protein is, however, less amenable to characterization by NMR than the LH2 complex, due to the structural heterogeneity of the pigment−protein oligomer. The BChl solid-state NMR signals have been assigned for hybrid LH1 dimer subunits (B820) and reassembled LH1 complexes that were reconstituted from the apopolypeptides of the carotenoidless mutant of *Rs. rubrum* and ^{13}C-labeled BChl a_p.[39,40] In these studies, one set of BChl signals was resolved for the LH1 α- and β-BChl's. In addition, for *Rb. sphaeroide*s LH1, a partial site-selective assignment of the polypeptide chemical shifts was obtained.[41] In contrast, for the highly homogeneously ordered peripheral LH2 complex, an almost complete assignment of the protein chemical shifts of the LH2 complex of *Rps. acidophila* has been accomplished, as well as a complete chemical shift assignment of the BChl signals, with a clear distinction between the B800 and B850 α- and β-BChl's.[2,42]

In this paper, we present the solid-state NMR signals and assignments of BChl *a* in intact LH1−RC core complexes of *Rps. acidophila*. The LH1 cofactor signals are assigned from homonuclear ^{13}C−^{13}C dipolar correlation data, and the spectra were recorded with the same instrument settings that were used for collecting the NMR data of LH2. This allows us to directly compare the observed LH1 NMR signals with the response from the LH2 complex, highlighting the differences between the BChl's in core and peripheral light-harvesting antennae that were isolated from the same *Rps. acidophila* 10050 strain. In addition, we are able to distinguish between the signals from the α- and β-BChl's, in contrast to earlier NMR studies on reconstituted LH1 complexes and their dimer subunits, where only one set of signals could be resolved. With the help of DFT shift calculations, we provide a first atomic view on the LH1 BChl ground-state structural and electronic interactions and propose that the antenna pigments may be optically tuned by shaping to perform their task of efficient light harvesting.

Materials and Methods

Uniformly [^{13}C, ^{15}N] isotopically enriched LH1−RC complexes were obtained by growing the photosynthetic purple bacteria *Rps. acidophila* 10050 anaerobically in light at 30 °C in a defined medium.[43] For label incorporation, ^{13}C-labeled succinic acid was prepared by a multistep synthesis starting from ^{13}C-labeled acetic acid. After 8 days of growing, cells were harvested by centrifugation at 4500 rpm for 10 min, resuspended in 20 mM Tris−HCl buffer (pH 8.0), and stored at −20 °C. For isolation of the membrane complexes, chromatophores were treated with 2% LDAO for 30 min at room temperature and then centrifuged for 10 min at 10 000 rpm at 4 °C to remove unsolubilized material. The supernatant was applied to discontinuous sucrose density gradients, and tubes were centrifuged at 55 000 rpm for 16 h at 4 °C. The membrane solution was resolved into three visible bands: the bottom band was the LH1−RC complex, the middle one the LH2 complex, and the upper band residual material and unbound pigments.

Isolated LH1−RC complexes were concentrated to a volume of ∼0.10 mL using centricon 100 kDa filters and transferred to a 4.0 mm CRAMPS rotor, containing approximately 10 mg of the sample. 2D homonuclear ^{13}C−^{13}C correlation spectra were recorded by radio frequency-driven dipolar recoupling (RFDR)[44] and proton-driven spin diffusion (PDSD) experiments. MAS NMR spectroscopy was performed with a Bruker AV-750 spectrometer equipped with a double channel CP-MAS probe head and with a ^{13}C radio frequency of 188 MHz. RFDR experiments were performed using mixing times of 2 and 5 ms, while the PDSD experiments were performed using various mixing times between 10 and 100 ms. For the PDSD experiments, proton decoupling was switched off during the spin diffusion mixing period to obtain ^{1}H-mediated transfer of ^{13}C polarization along the carbon network. All samples were cooled to 233 K, and the MAS spinning frequency was 13 kHz. The ^{13}COOH resonance of U-[^{13}C,^{15}N]-tyrosine·HCl at 172.1 ppm was used as an external chemical shift reference.

Density functional theory (DFT) and time-dependent DFT (TDDFT) calculations have been performed for several BChl *a* models to understand the effects on the electronic structure induced by different orientations of the C3 acetyl group defined by the C2−C3−C3^1−O3^1 dihedral angle ω and by the presence of a hydrogen bond. Model 1, fully optimized BChl *a*, served as a reference system for the other models; model 2 was obtained

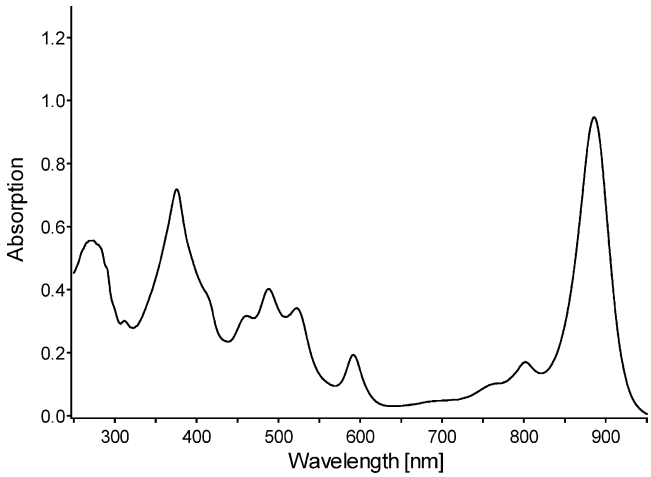

Figure 1. Room-temperature absorption spectrum of the [U−^{13}C,^{15}N] LH1−RC complex.

from model 1 by changing the angle $\omega = -180°$ to approximately $\omega = -90°$; model 3 has the same acetyl conformation as model 2 ($\omega = -90°$) and in addition a water molecule hydrogen bonded to the O3^1 oxygen; model 4 has the same acetyl conformation as model 1 ($\omega = -180°$) and in addition a water molecule hydrogen bonded to the O3^1 oxygen; and finally model 5 was obtained by optimizing the geometry from model 3, which leads to a dihedral angle of $\omega = -36°$. The phytyl tail of the BChl *a* was truncated at the esther group and saturated by a hydrogen atom in the model. The effect of this truncation on the electronic structure of the porphyrin ring is negligible.

For each model, we have computed the NMR chemical shifts and a few low-lying electronic excitation energies. All of the calculations were performed with the Gaussian 03 code[45] using the Becke's[46] and Lee−Young−Parr's[47] gradient-corrected functional (BLYP) in conjunction with a 6-31G(d,p) Gaussian basis set. This choice of functional and basis set is consistent with our previous calculations on the LH2 complex,[2] and tests with larger basis sets have demonstrated that chemical shift differences are sufficiently converged with the present basis set.[48]

Results

Figure 1 presents the room-temperature absorption spectrum of the [U−^{13}C−^{15}N] LH1−RC complex. The major peak in the near-infrared at 886 nm is the Q_y absorption maximum of the LH1 BChl's, and the small peak at 800 nm originates from the RC accessory BChl's. The shoulder at 760 nm is the absorption peak of the RC BPheo. Absorption spectra taken before and after the NMR experiments were identical, assuring sample integrity during the NMR measurements.

Figure 2 shows the RFDR ^{13}C−^{13}C correlation spectrum of the LH1−RC recorded with 2.45 ms mixing time, superimposed on a spectrum of uniformly labeled LH2 that was recorded with the same spinning frequency and at the same temperature. Correlation signals for the ^{13}C nuclei in the BChl *a* macrocycles are observed in the spectral region between 100 and 200 ppm and are well separated from the crowded protein region of the spectrum, between 0 and 70 ppm. The LH1 BChl's are abundant compared to the BChl's and BPheo of the RC, since 32 BChl's are present in LH1, compared with 4 BChl's and 2 BPheo in the RC. Hence, the observed BChl cross-peaks are predominantly the signals from the LH1 BChl's. We could assign many of the aromatic and aliphatic carbons of the LH1 BChl rings including the side chains. However, the C7, C7^1, C8^1, C17^1, C17^2, C17^3, C18, and C18^1 could not be assigned due to the strong overlap with signals from the protein in the crowded aliphatic region. In contrast, the good resolution of the C13^1−C13^2, C2^1−C2, C12^1−C12, and C3^2−C3^1 correlation signals allows for the unambiguous assignment of the C2, C2^1, C3, C3^1, C12, C12^1, C13^2, and C13^1 resonances and a direct comparison between the LH1 and LH2 NMR responses for these carbons. In the PDSD technique, the magnetization transfer is mediated by the ^{1}H nuclei, resulting in strong signals for the aliphatic carbons. The PDSD ^{13}C−^{13}C correlation spectra (data not shown) provided complementary information and were used to resolve the C5, C6, C19, and C20 carbon signals. While the C13^1−C13, C2^1−C2, and C12^1−C12 cross-peaks of the LH1 and LH2 spectra almost overlap, the C3^2−C3^1 cross-peaks are very different for the two complexes, as is shown in detail in Figures 3 and 4. Except for C13, two sets of signals could be distinguished for the LH1 ^{13}C resonances, reflecting differences in the conformation or local environment of the α- and β-BChl's. The line width of the BChl signals in the LH1 spectra is ∼1.5 ppm (220−230 Hz), compared to a line width of ∼1.0 ppm for the LH2 BChl data sets.[2]

Ring Current Shift Correction. The low-resolution structures of LH1 indicate that, analogous to the B850 ring in the LH2, the pyrrole rings I and III of neighboring BChl molecules overlap in the ring that is formed by the BChl dimers. Overlapping macrocycles give rise to ring current shifts, an effect in which a magnetic field component perpendicular to the plane of the aromatic system induces a ring current in the delocalized π electrons of the macroaromatic cycle, affecting the chemical shifts.[49] In previous work on the B850 α- and β-BChl's in LH2, local magnetic fields induced by the ring current effects were calculated by DFT using the geometries from the LH2 *Rps. acidophila* crystal structure.[2] For the LH2 complexes from *acidophila*, significant ring current shifts occur for the overlapping ring III of the α- and β-BChl macrocycles within the B850 dimer subunits and for the overlapping ring I macrocycles of adjacent BChl's between the subunits in the ring. This causes shielding of the C2, C2^1, C3, C3^1, and C3^2 carbon signals of ring I and of the C12^1 signals of ring III. For the LH1 BChl resonances, it is not known which set of signals belongs to the α-BChl's and which one to the β-BChl's, and there is no high-resolution crystal structure available to perform precise ring current shift calculations for this complex. Therefore, the average of the calculated ring current shifts for the corresponding ^{13}C of the LH2 B850 α- and β-BChl's was used to estimate the ring current shift correction for the ^{13}C nuclei of the LH1 BChl. Figure 5 provides the estimated shifts relative to the monomer in acetone-d_6 after ring current correction $|\Delta\sigma| \geq 1.0$ ppm, represented by blue circles (shielding effects) and red circles (deshielding effects) for the two sets of signals. The ^{13}C carbon shifts before and after performing the ring current correction are listed in Table 1.

Discussion

The broad lines of the LH1−RC BChl signals compared to LH2 reflect a larger degree of inhomogeneity within the LH1 complex, while still two sets of signals are resolved that distinguish the α- from the β-BChl's. It is not known whether *Rps. acidophila* LH1 forms closed or open rings. Opening of the ring would affect the NMR signals from the two outer BChl's of the "horseshoe"-shaped oligomer. This effect only occurs for 2 out of the 30 BChl's in a 15-mer "open ring" complex, and their signals are probably difficult to distinguish.

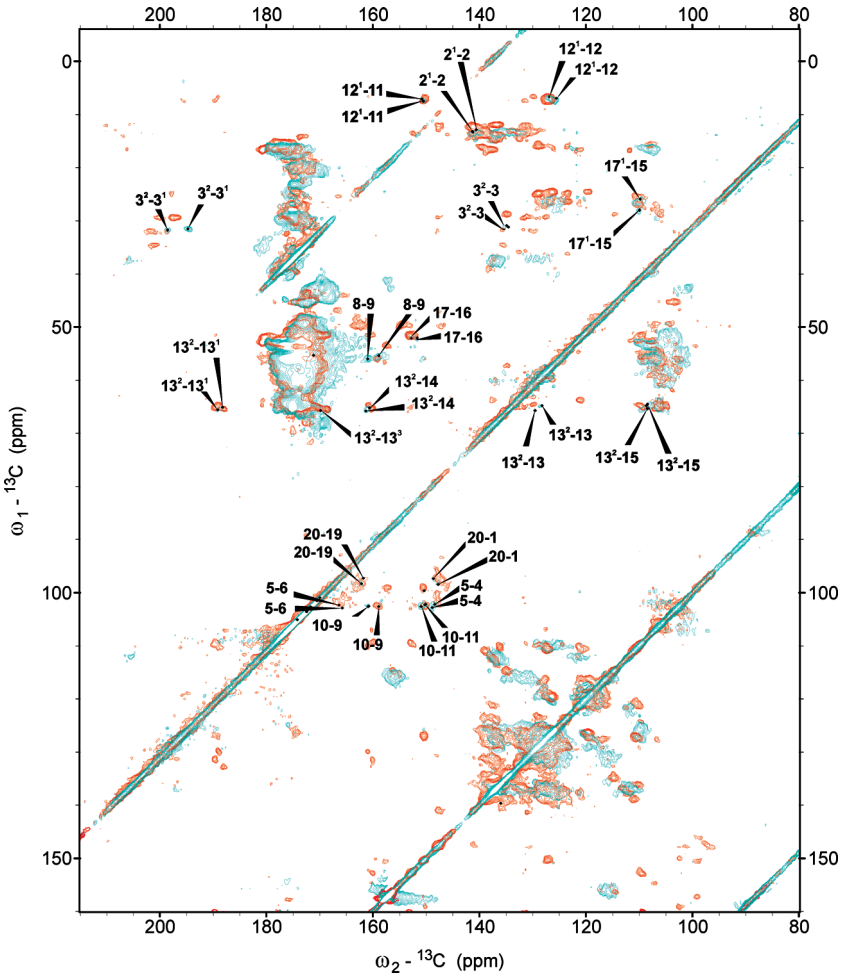

Figure 2. MAS 2D ^{13}C−^{13}C RFDR solid-state NMR spectrum of the [U−^{13}C,^{15}N] LH1−RC complex isolated from *Rps. acidophila* (in cyan), overlaid on the NMR spectrum of the [U−^{13}C,^{15}N] LH2 complex isolated from the same strain (in red). The data were obtained at 233 K with a spinning frequency of 13 kHz and a mixing time of 2.5 ms.

Opening of the ring would also increase the inhomogeneity resulting in broader NMR line shapes, but the effect would be similar to having a closed ellipse-shaped oligomer instead of a symmetrical ring.

Compared to monomeric BChl *a* in solution, both the LH1 and LH2 BChl's have a global pattern of large negative shifts around rings I and IV and a large positive shift for C12 at ring III. Significant differences between the two complexes are found for the C3 and C3^1, for C8, C9, and C10 (around ring II), and for the C13 carbons. The variations of the BChl ^{13}C chemical shifts can have different origins. They can be caused by changes in the shape of the macrocycles, electronic properties of the protein surrounding, ring current effects for overlapping rings I and III of the BChl macrocycles within and between BChl dimers, and hydrogen bonding of the 3^1-acetyl and 13^1-keto carbonyl groups. These BChl features are closely related to their optical absorbance properties. The Q_y absorbance of the LH1 BChl's is ∼100 nm red-shifted compared to BChl in solution and 50−70 nm red-shifted compared to the absorbance of the $\alpha\beta$ dimer subunits. The red shift of the Q_y absorbance of LH2 B850 BChl's compared to BChl in solution is ∼70 nm, and the Q_y absorbance red shift of the LH2 B800 BChl's is ∼20 nm. While a large part of the red shift of LH1 and LH2 B850 BChl's is explained by pigment−pigment excitonic interactions, also a significant part is attributed to interactions with the protein environment. Pigment−protein interactions are held responsible

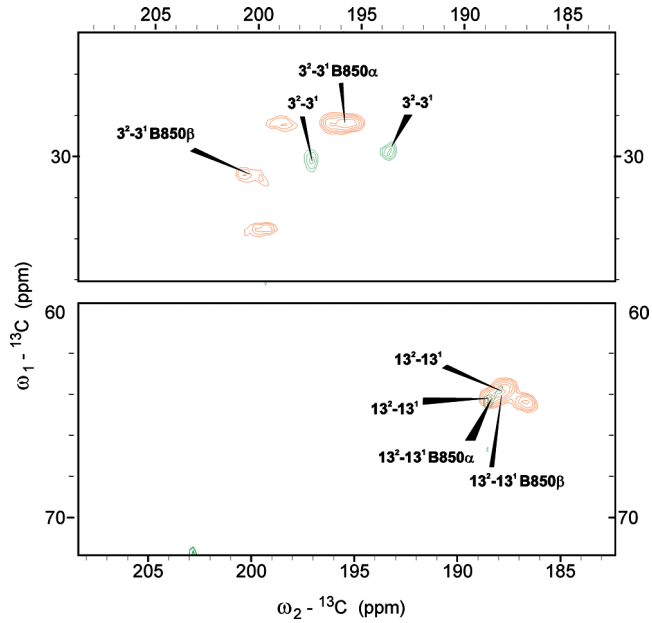

Figure 3. Comparison of the LH1 and LH2 B850 BChl 3-acetyl and 13-keto carbonyl chemical shifts. MAS 2D ^{13}C−^{13}C RFDR solid-state NMR spectrum of the LH1−RC complex (green), overlaid on the NMR spectrum of the LH2 complex (red). Assignments of the LH2 responses were taken from ref 2.

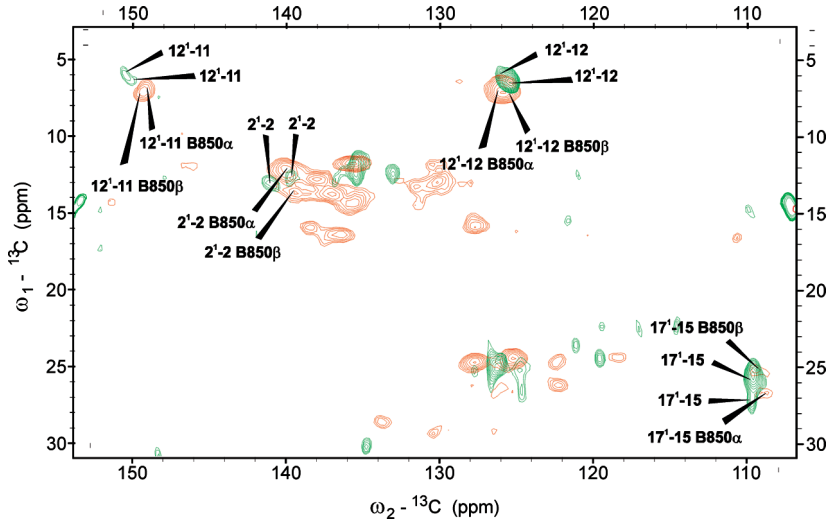

Figure 4. Comparison of the LH1 and LH2 B850 BChl side chain $C2^1$, $C12^1$ and $C17^1$ chemical shifts. MAS 2D $^{13}C-^{13}C$ RFDR solid-state NMR spectrum of the LH1−RC complex (green), overlaid on the NMR spectrum of the LH2 complex (red). Assignments of the LH2 responses were taken from ref 2.

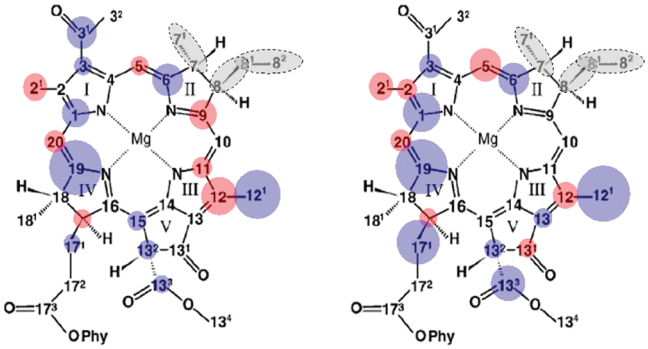

Figure 5. Estimated electronic shift changes after ring current correction represented by blue (negative, shielding) and red (positive, deshielding) circles for the α- and *β*-BChl's in the LH1−RC complex of *Rps. acidophila*. The sizes of the marks are proportional to the magnitudes of the electronic shift changes. The gray-filled areas were not assigned.

for the ∼20 nm red shift of B800 BChl's and for a 20−40 nm red shift of LH2 B850 and LH1 BChl's.[50,22]

We aim to relate the NMR chemical shift data to the ground-state pigment−protein interactions. Both the LH1 and LH2 BChl ground state electronic structures exhibit an electronic charge density pattern that is distributed globally over the macrocycles. In the earlier NMR study on LH2 BChl's, it was suggested that the BChl electronic ground-state polarization pattern might be induced by external effects from the protein surrounding, in particular the polarity of the protein environment. However, the B850 BChl's reside in a hydrophobic part of the protein with no charged groups in close vicinity. In this work, we consider the possibility that effects on the electronic structure are due to the protein-induced deformation of the BChl *a* molecules. Chlorophyll macrocycles are easily deformed at low energetic cost along the six lowest-frequency normal coordinates for out-of-plane and in-plane distortions of the macrocycle.[51] For photosynthetic reaction center complexes, it has become clear that the protein matrix can have strong control over the pigment conformation and that the NMR chemical shifts and electronic properties are quite sensitive to structural distortions.[52] In purple bacterial antenna and reaction center complexes, the protein geometric constraints induce very subtle physical distortions of BChl-ligating histidines that strongly alter their electronic properties.[37,38,48] NMR studies on chlorosome BChl *c* aggregates

TABLE 1: Chemical Shifts of the LH1 BChl Macrocycles[a]

	σ (ppm)		Δσ (ppm)		Δσ* (ppm)	
carbon	1	2	1	2	1	2
1	148.1	147.0	−2.9	−4.2	−2.5	−3.8
2	140.5	141.3	−1.7	−0.8	−0.3	+0.6
2^1	12.8	13.1	−0.7	−0.4	+1.5	+1.8
3	134.9	134.6	−2.7	−3.0	−1.5	−1.8
3^1	194.0	198.0	−5.3	−1.3	−4.1	−0.1
3^2	30.9	31.3	−2.0	−1.6	+0.1	+0.5
4	148.9	148.4	−1.3	−1.8	−0.1	−0.6
5	100.6	102.3	+1.0	+2.7	+1.3	+3.0
6	165.5	166.4	−3.4	−2.5	−3.4	−2.5
8	55.4	56.0	−0.2	+0.4	−0.2	+0.4
9	158.2	160.3	−0.3	+1.8	−0.3	+1.8
10	102.1	102.0	−0.3	−0.4	−0.1	−0.2
11	150.7	149.6	+1.2	+0.1	+1.2	+0.1
12	126.0	125.5	+2.1	+1.6	+2.8	+2.3
12^1	6.5	6.9	−5.4	−5.0	−3.9	−3.5
13	128.2		−2.3		−1.7	
13^1	187.8	188.2	−0.2	+0.2	+0.3	+0.7
13^2	64.3	65.1	−1.4	−0.6	−1.3	−0.5
13^3	170.3	168.5	−1.3	−2.9	−1.3	−2.9
14	160.5	160.6	−0.3	−0.2	−0.3	−0.2
15	108.7	109.4	−1.0	−0.3	−1.0	−0.3
16	151.4	152.2	−0.8	0.0	−0.8	0.0
17	51.5	51.4	+1.0	+0.9	+1.0	+0.9
17^1	27.6	25.9	−1.8	−3.5	−1.8	−3.5
19	161.8	161.6	−6.0	−5.7	−6.0	−5.7
20	97.0	97.5	+0.7	+1.2	+0.7	+1.2

[a] The isotropic ^{13}C chemical shifts (*σ*) of the two sets of BChl's in the LH1−RC complex of *Rps. acidophila* and the chemical shift differences between the monomeric BChl in acetone and the protein-bound BChl's, before (Δ*σ*) and after (Δ*σ**) subtraction of the estimated ring current shifts.

reveal two sets of signals for the macrocycle ^{13}C carbons of which the splitting can be explained by extended macrocycle distortions, arising from structural differences between the syn- and anti-conformers.[53] The impact of macrocycle deformations on the Q_y absorption maximum for the LH2 BChl has been addressed theoretically in a computational investigation by Neugebauer.[54] The effects of the distortion were quantified by comparing the single point analysis of the X-ray data set with a fully optimized model for the LH2 BChl's. In this way, a pronounced Q_y red shift of tens of nm for the X-ray structure calculations was found, relative to the fully optimized structures.

TABLE 2: DFT-Calculated Effect of BChl C3 Hydrogen Bonding and Out-of-Plane Rotation[a]

carbon	$\omega = -90°$ $\Delta\sigma$ (ppm)	H-bond, $\omega = -90°$ $\Delta\sigma$ (ppm)	H-bond, $\omega = -180°$ $\Delta\sigma$ (ppm)	H-bond, $\omega = 36°$ $\Delta\sigma$ (ppm)
2	−5.1	−5.1	+1.1	+4.0
2^1	−2.8	−2.9	+0.6	−2.0
3	+11.8	+10.7	+1.1	+8.6
3^1	+14.8	+19.4	+3.8	+5.8
3^2	+2.3	+2.8	−1.0	−1.5
4	−4.8	−5.1	−0.4	−2.3
5	−7.4	−7.6	−1.0	−7.3
6	−2.6	−2.5	0	−2.4
ΔQ_y	+0.079eV	+0.077eV	−0.012eV	+0.020eV
	−28.1 nm	−27.3 nm	+4.5 nm	−7.4 nm

[a] DFT-calculated effects of out-of-plane rotation of the C3-acetyl (ω) and of H-bonding to the $O3^1$. Column 1: calculated shifts for model 2 ($\omega = -90°$) relative to model 1 ($\omega = -180°$). Columns 2 and 3: calculated shifts for models 3 and 4 relative to model 1 presenting the effect of a hydrogen bond at $\omega = -90°$ and at $-180°$. Column 4: the effect of a hydrogen bond at $\omega = -36°$, calculated for model 5 with optimized geometry, relative to model 1.

Effects of H-Bonding and Out-of-Plane Rotation of the C3 Acetyl on the ^{13}C Chemical Shifts. The largest differences between LH1 and the LH2 B850 NMR responses are observed for C3 and $C3^1$. The C3 acetyl resonances should be sensitive to hydrogen bonding and side chain rotation. In a recent site-mutagenesis study on *sphaeroides* LH1, changes in the Q_y transition energies for different mutations were explained in terms of hydrogen bonding and C3 acetyl out-of-plane rotation.[36] By analogy to the LH2 structure of *Rs. molischianum*,[14] site-directed modification and modeling of the LH1 complex of *Rb. sphaeroides* suggest that in the LH1 complexes the 3^1-acetyls of LH1 α-BChl's are hydrogen bonded to tryptophans of the β-polypeptide and the 3^1-acetyls of LH1 β-BChl's are hydrogen bonded to tryptophans of the α-polypeptide.[55,56] The structurally symmetric H-bonding motif is thought to stabilize the $\alpha\beta$ subunits in the LH1 complex. The symmetric arrangement is different from the LH2 structure of *Rps. acidophila*, where the 3^1-acetyl of the α-B850 are H-bonded to the tryptophan of their α-polypeptide, while β-B850 BChl forms an intersubunit hydrogen bond to the tyrosine of the proceeding α-polypeptide, stabilizing the subunit oligomerization in a ring.[13]

To investigate the effect of out-of-plane rotation and hydrogen bonding on the C3 and $C3^1$ chemical shifts, DFT chemical shift calculations were performed for five different models (see Materials and Methods section). The chemical shift differences between the planar and out-of-plane conformations with and without a hydrogen bond are presented in Table 2. The effect of out-of-plane rotation on the global shift pattern is visualized in Figure 6, where the shifts of model 2 relative to model 1 (i.e., the effect of 90° out-of-plane rotation) are mapped onto the BChl macrocycle structure. In addition, the excited state energies of the lowest optical Q_y transition were calculated by TDDFT for the five model structures, and the shifts of the Q_y maxima with respect to the reference value of model 1 are listed in Table 2. The results show that out-of-plane rotation of the C3 acetyl affects mostly the C3, $C3^1$, C2, C4, and C5 responses, resulting in large downfield shifts for C3 and $C3^1$ (12−14 ppm for −90° rotation) and a large ∼7 ppm upfield shift for C5. The effect of hydrogen bonding is smaller and localized at the $C3^1$, resulting in a ∼4 ppm downfield shift.[1] Out-of-plane rotation results in large blue shifts of the Q_y absorption band (∼30 nm for −90° rotation), in line with earlier calculations by Gudowska-Nowak et al.[57] The effect of hydrogen bonding on the Q_y absorbance maximum is also smaller than the effect of out-of-plane rotation, resulting in a 4.5 nm red shift for a BChl in planar conformation and less than 1 nm red shift for BChl with the C3 held at $\omega = -90°$ out-of-plane.

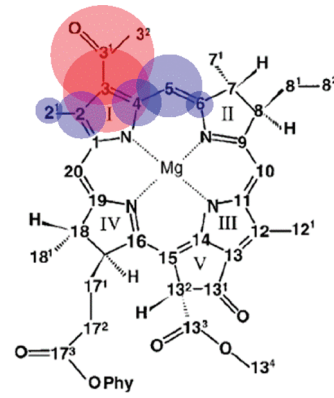

Figure 6. DFT-calculated shift patterns for the effect of 90° out-of-plane rotation of the C3 acetyl. The calculated shifts for model 2 ($\omega = -90°$) relative to model 1 ($\omega = -180°$) are presented by blue (negative, shielding) and red (positive, deshielding) circles, with the sizes proportional to the magnitude of the shift changes.

We wanted to know to which extent the predicted effects of out-of-plane rotation and hydrogen bonding to the C3 acetyl could explain the observed chemical shifts. Therefore, we first take a look at the NMR data of LH2 obtained in an earlier study,[2] of which the degree of C3 out-of-plane rotation and hydrogen bond patterns are known from the high-resolution X-ray structure. The predicted shift effect of hydrogen bonding is consistent with the observed downfield shift of the $C3^1$ signal of the LH2 βB850 BChl that forms a strong hydrogen bond between αY44 and the C3 acetyl and of the observed downfield shift of the $C3^1$ signal of the LH2 B800 BChl. Although the αB850 is also thought to form a weak hydrogen bond between $O3^1$ and αW45, this effect is not visible in the chemical shifts and the αB850 $C3^1$ signal matches the shift observed for monomeric BChl *a* in solution.[13] In the crystal structures of the LH2 of *Rps. acidophila*, C3 acetyl, dihedral angles of 194°/159°[13] and −166°/156°[35] have been observed for the α/β-B850 BChl's, which conforms to moderate out-of-plane rotation. However, the observed chemical shift patterns for the C3, $C3^1$, and C5 of the LH2 BChl's do not match with the predicted results for out-of-plane rotation according to Table 2 and the shift pattern drawn in Figure 6.

According to the LH2 *Rps. acidophila* structure, none of the BChl's is fully planar and the B850 β-BChl is significantly distorted with respect to αB850 and B800 and in a saddle conformation with a bowing along the long axis (between rings I and III).[13] Raman experiments showed a 10 cm^{-1} splitting of

the R_5 band[33] that is sensitive to the C_a-N-C_a angles in porphyrin molecules, and it was concluded that the LH2 BChl's are in restrained conformations with a difference between the α- and β-polypeptide-bound BChl. The electronic structures of the B850 BChl's derived from their NMR chemical shifts both differ from monomeric BChl *a* in solution, with large negative patterns around rings I and IV. In the absence of other explanations, we propose that these differences to a large extent can be ascribed to macrocycle deformation that seems to predominate over the localized effects due to a rotation of the side chain. This presumes that both the α- and β-BChl's are distorted, although the more pronounced distortional features of the β-BChl in the LH2 X-ray structure might be expressed by the relative shift differences between the α- and β-BChl's. The B850 α- and β-BChl electronic structures are similar around rings I, III, and IV but significantly differ around ring II, where the α-BChl has a pattern of many negative shifts and the β-BChl has positive shifts at the $C8^1$ and $C8^2$ atoms. In the absence of point charges in the close vicinity, these effects are likely introduced by differences in the α- and β-BChl conformations and might relate to the observed splitting of the R_5 Raman mode.

A comparison of Figure 5 with Figure 6 clearly shows that the observed shift patterns of the LH1 BChl's do not represent the effects of out-of-plane rotation of the C3 acetyl. According to the $C3^1$ shifts, no strong hydrogen bonds are formed, since this would give a positive (downfield) shift. One of the two BChl $C3^1$ responses has a negative shift, while the other is very similar to the $C3^1$ response observed for monomeric BChl *a* in solution. In analogy to the $C3^1$ response of the αB850 BChl, the latter LH1 BChl C3 acetyl may form a weak hydrogen bond of which the effect is not visible in the NMR. For both sets of the LH1 BChl responses, the C3 signals are shifted upfield. Interestingly, similar to one of the *Rps. acidophila* LH1 BChl C3 and $C3^1$ responses, a pattern of upfield $C3^1$ and C3 shifts was observed for the BChl's in reconstituted LH1 of *Rs. rubrum*,[40] while a large positive $C3^1$ shift indicative of a strong hydrogen bond was observed for its B820 subunits.[39] This is in agreement with the observations from Raman experiments that the hydrogen bond to the 3^1-acetyl carbonyl is strengthened upon dissociation of the LH1 complex into B820 subunits.[58]

We assume that also for the LH1 the global shift patterns reflect the effects of macrocycle deformation that predominate over the C3 side chain effects. The LH1 BChl's also have electronic structures that differ from monomeric BChl *a* in solution with negative patterns around rings I and IV, similar to the BChl's of LH2, presuming structural deformation of both BChl's. Like for LH2, there are significant differences between the electronic structures of the LH1 α- and β-bound BChl's, but these are more evenly distributed over the macrocycle rings, with the largest differences for rings I and II. This may explain why in Raman experiments comparing the distorted features of the LH1 to the LH2 B850 BChl's, for LH1 BChl's additional splitting of the R_1 band was observed.[33]

Hydrogen Bonding to the 13-Keto Carbonyl. In addition to the BChl 3-acetyl, hydrogen bonds can be formed to the 13-keto carbonyl groups. Small downfield shifts are observed for the NMR response of one of the LH1 13^1-keto carbonyls and for the LH2 αB850 BChl that match with the formation of weak hydrogen bonds. The possibility of weak H-bonding of the keto carbonyls of LH2 BChl's was suggested on the basis of the small downshift of the C═O stretching mode.[30] In Raman data of *rubrum* and *sphaeroides* LH1, hydrogen bonding of the 13^1-keto carbonyls was observed and for *sphaeroides* LH1 it has been proposed that they are H-bonded to the imidazoles of the adjacent BChl-coordinating His in the subunits.[55] The BChl NMR responses of *acidophila* LH1, however, show $C13^2-C13^1$ cross-peaks that are remarkably similar to the responses of LH2 (see Figure 3, lower panel) and according to which only one of the two BChl keto carbonyls forms an H-bond.

Disruption of the H-bond to the keto carbonyl does not cause spectral shifts[30,31] but affects the thermal stability. On the basis of LH2 mutational studies, it was proposed that instead of spectral tuning, H-bonding the $O13^1$ of beta-ligated (B)Chl's has a structural role in stabilizing pigment−protein assemblies.[59] According to the crystal structure of *acidophila* LH2, H-bonding of the BChl keto carbonyl to the His imidazoles as proposed for LH1 is unlikely.[12] A previous NMR study provided evidence, though, that the His imidazoles in *acidophila* LH2 are hydrogen bonded,[48] and according to DFT modeling, likely candidates for H-bonding to the His imidazoles are the alanine carbonyls at position −4 (Wawrzyniak, personal communication, the numbering is relative to the coordinating His position). This implies that the residues at position −4 lock the orientation of the His by forming H-bonds both to its main chain via the $C{=}O_{i-4}\cdots NH_i$ α-helical stabilizing H-bond and to its imidazole side chain. The α-residue at the −4 position has been subjected to mutation in *sphaeroides* LH2[30,34] with effects on the stability. This was explained by disruption of the β-BChl keto carbonyl H-bond to the hydroxyl of a serine residue at this position.[30] Combining the results, there appears to be a connected network of LH2 stabilizing interactions involving His−BChl ligation combined with H-bonding of the BChl keto carbonyls and/or the His imidazoles to the residues at position −4.

His−BChl Interactions Affecting the $C12^1$ Chemical Shifts. Other ^{13}C shifts that can be explained by specific protein−cofactor interactions are the shifts observed for the $C12^1$. Both the LH1 and B850 BChl's of LH2 have a large negative shift at $C12^1$, which differs from the LH2 B800 BChl's in which the $C12^1$ has a positive shift. Histidine-labeled LH2 experiments in combination with DFT calculations revealed that the B850 BChl-coordinating His in LH2 carry partial positive charge, induced by electron transfer to the coordinating BChl that carry a net negative charge.[48] In the B850 BChl dimer, the His side chains are close to the $C12^1$ and $O13^1$ of the opposite BChl. The presence of the His partial positive charge could explain the partial negative charge around $C12^1$ in the B850 BChl's that polarizes the macrocycle around ring III. The LH1 BChl's are also His-coordinated and a similar effect could produce negative shifts for the LH1 BChl $C12^1$ signals.

Consequences for the Protein Contribution to the BChl Q_y Red Shift. The DFT analyses illustrate how the chemical shift variations relate to pigment−protein interactions that affect the optical spectral properties of the Q_y absorbance band. There are several protein-induced parameters that in theory could affect the BChl optical spectral properties: (1) shaping of porphyrin macrocycles can induce spectral shifts up to tens of nm;[60] (2) rotation of the C3 acetyl can cause up to ∼30 nm blue shift for 90° rotation[57] and could explain part of the observed blue shift in LH3 complexes; (3) hydrogen bonding of the 3^1-acetyl has proven to induce a red shift of the Q_y absorption band[26−29] and H-bonding to the 13^1-keto-carbonyl would theoretically induce a blue shift, but experimentally, no spectral shifts were observed upon disruption of this bond;[30] (4) Mg-ligation to His induces a 3 nm red shift;[61] and (5) point charges in the vicinity of ring I or III of the BChl macrocycles can introduce Q_y spectral shifts[61] and account for part of the observed red shift in LH2 B800 BChl's.[28]

Point Charges. The BChl−Mg coordinating His of LH2, which contain partial positive charge,[48] reside in van der Waals distance to ring III of the macrocycle of the opposite BChl and affect the Q_y absorbance band, probably by inducing a blue shift, since a partial positive charge would counteract the transition dipole. The observed negative $C3^1$ shift for one of the LH1 BChl's could be caused by local positive charges in close vicinity. This would in fact introduce a Q_y red shift effect that is not present in LH2.

Mg Ligation. Ligation of the BChl Mg to His will produce a small red shift. DFT calculations on the His−BChl charge-transfer effect have estimated that the charge transfer only has a small effect on the Q_x absorbance band.[48]

Hydrogen Bonding to the 3^1-Acetyl or 13^1-Keto-Carbonyl. The $C13^1$ chemical shifts suggest that weak hydrogen bonds are formed to $O13^1$ in LH1 and LH2 that may induce a blue shift, although there has been no experimental evidence of the relation between H-bonding to this group and spectral shifts. One of the LH1 BChl's could be hydrogen bonded to the $O3^1$, inducing a red shift up to ∼5 nm. According to the X-ray structure, both LH2 B850 BChl's are H-bonded to their C3 acetyl, although in the NMR this is only reflected in the β-BChl $C3^1$ shifts.

Rotation of the C3 Acetyl. None of the LH2 and LH1 BChl's have a typical pattern of downfield-shifted C3 and $C3^1$ responses combined with upfield shifted C5 responses, indicative of significant out-of plane rotation of its C3 acetyls. In contrast, large negative shifts are observed for the C3 responses (combined with positive shifts for C5), in particular for the LH2 B850 BChl's. This does not exclude out-of-plane rotation of the C3 acetyl but suggests that other distortional effects are dominant.

Shaping of the Porphyrin Macrocycles. The LH1 and LH2 B850 BChl's have global shift patterns that differ from monomeric BChl *a* in solution and that are likely induced by macrocycle deformation. For both types of complexes, there are pronounced differences between the patterns of the α- and β-bound BChl's. We propose that deformations involving the macrocycle rings, perhaps accompanied by local charges near the LH1 BChl, can significantly contribute to the protein-induced part of the BChl Q_y red shift in LH1 and LH2 complexes and can lead to dissimilar LH2 and LH1 Q_y absorbance bands.

Conclusions

A comprehensive assignment of ^{13}C NMR signals of the LH1 BChl macrocycles in intact, $^{13}C-^{15}N$ enriched purple bacterial LH1−RC core complexes is attained and compared to the NMR responses of the BChl's in related LH2 complexes. This provides an atomic-level view on the differences between the BChl's in core and peripheral antennae of the same species and goes beyond the limitations of crystallographic data obtained from the purple bacterial core antennae. The splitting of the BChl carbon responses expresses the asymmetry between the α- and β-BChl's in LH1, while the broader line shapes in the LH1 ^{13}C NMR spectra relative to LH2 indicate that the LH1 core complex is less homogeneous than the peripheral LH2 complex. While DFT calculations confirm that hydrogen bonding and in particular out-of-plane rotation of the C3 acetyl side chain have a significant effect on the chemical shifts and the BChl Q_y absorption maximum, the NMR observed shift patterns seem to be dominated by extensive macrocycle deformations that could also significantly contribute to the Q_y red shift.

In a sterically crowded pigment−protein complex, a limited number of structural conformations is energetically accessible to the chlorophylls. This allows for specific tuning of the light-harvesting properties through localized structural perturbations. Now that such elementary design properties can be mapped by NMR, it may prove advantageous to use similar principles for the design of nanostructured artificial systems for harnessing solar energy.

Acknowledgment. A.P. was supported by a VENI grant 700.55.408 from The Netherlands Organization of Scientific Research. We acknowledge the support from the Stichting Nationale Computerfaciliteiten (NCF-NWO) for the use of the SARA supercomputer facilities.

References and Notes

(1) Pandit, A.; Wawrzyniak, P. K.; van Gammeren, A. J.; Buda, F.; Ganapathy, S.; de Groot, H. J. M. *Biochemistry* **2010**, *49*, 478.
(2) van Gammeren, A. J.; Buda, F.; Hulsbergen, F. B.; Kiihne, S.; Hollander, J. G.; Egorova-Zachernyuk, T. A.; Fraser, N. J.; Cogdell, R. J.; de Groot, H. J. M. *J. Am. Chem. Soc.* **2005**, *127*, 3213.
(3) Cogdell, R. J.; Gall, A.; Kohler, J. *Q. Rev. Biophys.* **2006**, *39*, 227.
(4) Pandit, A.; Visschers, R. W.; van Stokkum, I. H. M.; Kraayenhof, R.; van Grondelle, R. *Biochemistry* **2001**, *40*, 12913.
(5) Pandit, A.; van Stokkum, I. H. M.; Georgakopoulou, S.; van der Zwan, G.; van Grondelle, R. *Photosynth. Res.* **2003**, *75*, 235.
(6) Parkes-Loach, P. S.; Sprinkle, J. R.; Loach, P. A. *Biochemistry* **1988**, *27*, 2718.
(7) Pandit, A.; Ma, H. R.; van Stokkum, I. H. M.; Gruebele, M.; van Grondelle, R. *Biochemistry* **2002**, *41*, 15115.
(8) Reynolds, N. P.; Janusz, S.; Escalante-Marun, M.; Timney, J.; Ducker, R. E.; Olsen, J. D.; Otto, C.; Subramaniam, V.; Leggett, G. J.; Hunter, C. N. *J. Am. Chem. Soc.* **2007**, *129*, 14625.
(9) Suemori, Y.; Fujii, K.; Ogawa, M.; Nakamura, Y.; Shinohara, K.; Nakagawa, K.; Nagata, M.; Iida, K.; Dewa, T.; Yamashita, K.; Nango, M. *Colloids Surf., B* **2007**, *56*, 182.
(10) Ochiai, T.; Asaoka, T.; Kato, T.; Osaka, S.; Dewa, T.; Yamashita, K.; Gardiner, A. T.; Hashimoto, H.; Nango, M. *Photosynth. Res.* **2008**, *95*, 353.
(11) Sundstrom, V.; Pullerits, T.; van Grondelle, R. *J. Phys. Chem. B* **1999**, *103*, 2327.
(12) Papiz, M. Z.; Prince, S. M.; Howard, T.; Cogdell, R. J.; Isaacs, N. W. *J. Mol. Biol.* **2003**, *326*, 1523.
(13) Prince, S. M.; Papiz, M. Z.; Freer, A. A.; McDermott, G.; HawthornthwaiteLawless, A. M.; Cogdell, R. J.; Isaacs, N. W. *J. Mol. Biol.* **1997**, *268*, 412.
(14) Koepke, J.; Hu, X. C.; Muenke, C.; Schulten, K.; Michel, H. *Structure* **1996**, *4*, 581.
(15) Roszak, A. W.; Howard, T. D.; Southall, J.; Gardiner, A. T.; Law, C. J.; Isaacs, N. W.; Cogdell, R. J. *Science* **2003**, *302*, 1969.
(16) Richter, M. F.; Baier, J.; Prem, T.; Oellerich, S.; Francia, F.; Venturoli, G.; Oesterhelt, D.; Southall, J.; Cogdell, R. J.; Kohler, J. *Proc. Natl. Acad. Sci. U.S.A.* **2007**, *104*, 6661.
(17) Tunnicliffe, R. B.; Ratcliffe, E. C.; Hunter, C. N.; Williamson, M. P. *FEBS Lett.* **2006**, *580*, 6967.
(18) Wang, Z. Y.; Suzuki, H.; Kobayashi, M.; Nozawa, T. *Biochemistry* **2007**, *46*, 3635.
(19) Scheuring, S.; Seguin, J.; Marco, S.; Levy, D.; Robert, B.; Rigaud, J. L. *Proc. Natl. Acad. Sci. U.S.A.* **2003**, *100*, 1690.
(20) Karrasch, S.; Bullough, P. A.; Ghosh, R. *EMBO J.* **1995**, *14*, 631.
(21) Fotiadis, D.; Qian, P.; Philippsen, A.; Bullough, P. A.; Engel, A.; Hunter, C. N. *J. Biol. Chem.* **2004**, *279*, 2063.
(22) Cogdell, R. J.; Howard, T. D.; Isaacs, N. W.; McLuskey, K.; Gardiner, A. T. *Photosynth. Res.* **2002**, *74*, 135.
(23) Scheuring, S.; Sturgis, J. N. *Photosynth. Res.* **2009**, *102*, 197.
(24) Qian, P.; Bullough, P. A.; Hunter, C. N. *J. Biol. Chem.* **2008**, *283*, 14002.
(25) Sener, M.; Hsin, J.; Trabuco, L. G.; Villa, E.; Qian, P.; Hunter, C. N.; Schulten, K. *Chem. Phys.* **2009**, *357*, 188.
(26) Fowler, G. J. S.; Sockalingum, G. D.; Robert, B.; Hunter, C. N. *Biochem. J.* **1994**, *299*, 695.
(27) Sturgis, J. N.; Jirsakova, V.; Reisshusson, F.; Cogdell, R. J.; Robert, B. *Biochemistry* **1995**, *34*, 517.
(28) Gall, A.; Fowler, G. J. S.; Hunter, C. N.; Robert, B. *Biochemistry* **1997**, *36*, 16282.
(29) Sturgis, J. N.; Robert, B. *J. Phys. Chem. B* **1997**, *101*, 7227.
(30) Braun, P.; Vegh, A. P.; von Jan, A.; Strohmann, B.; Hunter, C. N.; Robert, B.; Scheer, H. *Biochim. Biophys. Acta* **2003**, *1607*, 19.
(31) Kwa, L. G.; Garcia-Martin, A.; Vegh, A. P.; Strohmann, B.; Robert, B.; Braun, P. *J. Biol. Chem.* **2004**, *279*, 15067.

(32) Gentemann, S.; Nelson, N. Y.; Jaquinod, L.; Nurco, D. J.; Leung, S. H.; Medforth, C. J.; Smith, K. M.; Fajer, J.; Holten, D. *J. Phys. Chem. B* **1997**, *101*, 1247.

(33) Lapouge, K.; Naveke, A.; Gall, A.; Ivancich, A.; Seguin, J.; Scheer, H.; Sturgis, J. N.; Mattioli, T. A.; Robert, B. *Biochemistry* **1999**, *38*, 11115.

(34) Silber, M. V.; Gabriel, G.; Strohmann, B.; Garcia-Martin, A.; Robert, B.; Braun, P. *Photosynth. Res.* **2008**, *96*, 145.

(35) McLuskey, K.; Prince, S. M.; Cogdell, R. J.; Isaacs, N. W. *Biochemistry* **2001**, *40*, 8783.

(36) Uyeda, G.; Williams, J. C.; Roman, M.; Mattioli, T. A.; Allen, J. P. *Biochemistry* **2010**, *49*, 1146.

(37) Alia, A.; Matysik, J.; de Boer, I.; Gast, P.; van Gorkom, H. J.; de Groot, H. J. M. *J. Biomol. NMR* **2004**, *28*, 157.

(38) Alia, A.; Wawrzyniak, P. K.; Janssen, G. J.; Buda, F.; Matysik, J.; de Groot, H. J. M. *J. Am. Chem. Soc.* **2009**, *131*, 9626.

(39) Wang, Z. Y.; Muraoka, Y.; Shimonaga, M.; Kobayashi, M.; Nozawa, T. *J. Am. Chem. Soc.* **2002**, *124*, 1072.

(40) Umetsu, M.; Kadota, T.; Wang, Z. Y.; Tanaka, Y.; Adschiri, T.; Nozawa, T. *Chem. Lett.* **2005**, *34*, 940.

(41) Huang, L.; McDermott, A. E. *Biochim. Biophys. Acta* **2008**, *1777*, 1098.

(42) van Gammeren, A. J.; Hulsbergen, F. B.; Hollander, J. G.; de Groot, H. J. M. *J. Biomol. NMR* **2005**, *31*, 279.

(43) Egorova-Zachernyuk, T. A.; Hollander, J.; Fraser, N.; Gast, P.; Hoff, A. J.; Cogdell, R.; de Groot, H. J. M.; Baldus, M. *J. Biomol. NMR* **2001**, *19*, 243.

(44) Bennet, A. E.; Ok, J. K.; Griffin, R. G.; Vega, S. *J. Chem. Phys.* **1992**, *96*, 8624.

(45) Frisch, M. J.; Trucks, G. W.; Schlegel, H. B.; Scuseria, G. E.; Robb, M. A.; Cheeseman, J. R.; Montgomery, J. A.; Vreven, T.; Kudin, K. N.; Burant, J. C. *Gaussian 03*, revision C.02; Gaussian, Inc.: Wallingford, CT, 2004.

(46) Becke, A. D. *Phys. Rev. A* **1988**, *38*, 3098.

(47) Lee, C. T.; Yang, W. T.; Parr, R. G. *Phys. Rev. B* **1988**, *37*, 758.

(48) Wawrzyniak, P. K.; Alia, A.; Schaap, R. G.; Heemskerk, M. M.; de Groot, H. J. M.; Buda, F. *Phys. Chem. Chem. Phys.* **2008**, *10*, 6971.

(49) Giessner-Prettre, C.; Pullman, B. *J. Theor. Biol.* **1971**, *31*, 287.

(50) Sturgis, J. N.; Robert, B. *Photosynth. Res.* **1996**, *50*, 5.

(51) Jentzen, W.; Song, X. Z.; Shelnutt, J. A. *J. Phys. Chem. B* **1997**, *101*, 1684.

(52) Daviso, E.; Prakash, S.; Alia, A.; Gast, P.; Neugebauer, J.; Jeschke, G.; Matysik, J. *Proc. Natl. Acad. Sci. U.S.A.* **2009**, *106*, 22281.

(53) Ganapathy, S. Ph.D. Thesis, *Bridging the gap between natural and artificial light-harvesting*; Leiden University, Leiden, The Netherlands, 2008.

(54) Neugebauer, J. *J. Phys. Chem. B* **2008**, *112*, 2207.

(55) Olsen, J. D.; Sturgis, J. N.; Westerhuis, W. H. J.; Fowler, G. J. S.; Hunter, C. N.; Robert, B. *Biochemistry* **1997**, *36*, 12625.

(56) Hu, X.; Schulten, K. *Biophys. J.* **1998**, *75*, 683.

(57) Gudowska-Nowak, E.; Newton, M. D.; Fajer, J. *J. Phys. Chem.* **1990**, *94*, 5795.

(58) Visschers, R. W.; R., v. G.; Robert, B. *Biochim. Biophys. Acta* **1993**, *1183*, 369.

(59) Garcia-Martin, A.; Kwa, L. G.; Strohmann, B.; Robert, B.; Holzwarth, A. R.; Braun, P. *J. Biol. Chem.* **2006**, *281*, 10626.

(60) Haddad, R. E.; Gazeau, S.; Pecaut, J.; Marchon, J. C.; Medforth, C. J.; Shelnutt, J. A. *J. Am. Chem. Soc.* **2003**, *125*, 1253.

(61) Hanson, L. K.; Fajer, J.; Thompson, M. A.; Zerner, M. C. *J. Am. Chem. Soc.* **1987**, *109*, 4728.

JP100688U